

Differential movement and movement bias models for marine protected areas

Jessica Langebrake · Louise Riotte-Lambert ·
Craig W. Osenberg · Patrick De Leenheer

Received: 1 October 2010 / Revised: 25 November 2010
© Springer-Verlag 2011

Abstract Marine protected areas (MPAs) are promoted as a tool to protect over-fished stocks and increase fishery yields. Previous models suggested that adult mobility modified effects of MPAs by reducing densities of fish inside reserves, but increasing yields (i.e., increasing densities outside of MPAs). Empirical studies contradicted this prediction: as mobility increased, the relative density of fishes inside MPAs (relative to outside) increased or stayed constant. We hypothesized that this disparity between theoretical and empirical results was the result of differential movement of fish inside versus outside the MPA. We, therefore, developed a model with unequal and discontinuous diffusion, and analyzed its steady state and stability. We determined the abundance in the fishing grounds, the yield, the total abundance and the log ratio at steady-state and examined their response to adult mobility (while keeping the relative inequity in the diffusion constant). Abundance in the fishing grounds and yield increased, while total abundance and log-ratio decreased, as mobility increased. These results were all qualitatively consistent with the previous models assuming uniform diffusivity. Thus, the mismatch between empirical and theoretical results must result

This paper is dedicated to Simon Levin, on the occasion of his 70th birthday.

J. Langebrake · P. De Leenheer (✉)
Department of Mathematics, University of Florida, Orlando, FL, USA
e-mail: deleenhe@ufl.edu

J. Langebrake
e-mail: jessica.langebrake@gmail.com

L. Riotte-Lambert
Département de Biologie, Ecole Normale Supérieure, Lyon Cedex, France
e-mail: riotte@horus.ens.fr

C. W. Osenberg
Department of Biology, University of Florida, Orlando, FL, USA
e-mail: osenberg@ufl.edu

from other processes or other forms of differential movement. Therefore, we modified our original model by assuming that species located on the boundary of the MPA will preferentially move towards the MPA. This localized movement bias model gives rise to steady state profiles that can differ radically from the profiles in the unbiased model, especially when the bias is large. Moreover, for sufficiently large bias values, the monotonicity of the four measures with increased mobility is reversed, when compared with our original model. Thus, the movement bias model reconciles empirical data and theoretical results.

Mathematics Subject Classification (2000) 34A36 · 34B18 · 34B60 · 35B30 · 35K57 · 35Q92

1 Introduction

Overfishing has reduced marine fish stocks and degraded habitats (Sale et al. 2005; Selig and Bruno 2010). As a consequence, fisheries management has become a major economic and environmental challenge. Marine reserves [or marine protected areas (MPAs)] are frequently advocated as an efficient management tool to restore habitats and protect over-harvested stocks (Hilborn 2003; Hilborn et al. 2004; Sale et al. 2005; Claudet et al. 2008; Selig and Bruno 2010). MPAs offer two potential benefits. First, they can locally increase the densities of harvested species (Hilborn 2003; Claudet et al. 2010), but see (Osenberg et al. 2006). Secondly, they can increase fishing yields outside of the marine reserve via spillover and/or larval export (Roberts et al. 2001; Sale et al. 2005; Goñi et al. 2008) (spillover is defined as the net movement of adult fish from the reserve to the fishing grounds, which results in a biomass export).

Despite the evidence supporting local benefits of MPAs, uncertainties remain (Hilborn et al. 2004; Sale et al. 2005; Osenberg et al. 2006). For example, theoretical studies have suggested that the local effectiveness of an MPA decreases as adult mobility increases (Gerber et al. 2003; Malvadkar and Hastings 2008; Pérez-Ruzafa et al. 2008; Moffitt et al. 2009; West et al. 2009). Empirical data do not support this theoretical expectation. For example, in a recent meta-analysis of Mediterranean MPAs (Claudet et al. 2010) calculated the relative densities of fish inside versus outside MPAs, and compared the results for species with low, medium or high adult mobility. In contrast to the theoretical expectation, they found that the density of fish inside of MPAs (relative to outside) did not decrease as mobility increased. To explain their surprising results, Claudet et al. (2010) suggested that mobile species could benefit more from MPAs than expected if they biased their movement in favor of the reserve and such a bias could result if the MPA altered habitat availability or quality (Selig and Bruno 2010) and the target species preferred this modification.

In contrast to the expected negative relationship between increased local effects (one goal of MPAs) and mobility, models generally indicate that fishing yields (the second goal) should increase with fish mobility as a result of increased spillover (Gerber et al. 2003; Le Quesne and Codling 2009; Moffitt et al. 2009). There are no available empirical data to evaluate whether this expectation also is contradicted.

The conflict between empirical and theoretical predictions about the relationship between mobility and local effects of MPAs, as well as the importance of spillover for producing increased fisheries yields, suggests that we need to examine the effects of mobility in new ways. The main purpose of this paper is to propose several models that could reconcile model predictions and empirical results.

We will start by introducing a model that examines how differential movement inside versus outside the MPA can affect the efficacy of MPAs. To date, there have been only limited studies of this phenomenon. For example, [Rodwell et al. \(2003\)](#) developed a two patch model where adult movement was described by an annual transfer from the most populated patch to the other, i.e. from the reserve to the fishing grounds. We model fish movement as a diffusion process and assume that the diffusion parameter is smaller inside the reserve than outside. Mathematically, the model is a boundary value problem with piecewise constant parameters in different spatial regions. On each region, the steady state equation is linear so that it can be solved explicitly. The solutions need to be matched at the interface of the regions, a technique that is well known, see for instance [Shigesada et al. \(1986\)](#), [Cantrell and Cosner \(1999\)](#). Then, we investigate how differential diffusion affects the expected benefits of MPAs. We focus on four measures: abundance of fish in the fishing grounds (i.e. the amount of fish in the fished area), total abundance (i.e. the amount of fish contained in the MPA and fished area combined), the local effect (i.e., log of the ratio of the density inside versus outside of the MPA, which is a common measure of the effect of an MPA), and fisheries yield (i.e., the amount of fish caught by fishers per unit of time). We will show that if the two diffusion parameters are scaled as mobility increases, yet their ratio remains constant, the measures vary in a way that is in accordance with the theoretical predictions from traditional models.

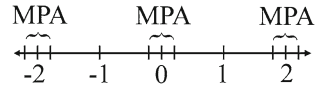
Next, we introduce a model that incorporates a movement bias towards the MPA which is localized to the MPA boundary. It arises as the limit of a random walk model where the random walk is only truly random away from the boundary, but biased on the boundary. We show that there is a critical value for the bias parameter that controls the dependence of the four measures on increased mobility. For small bias, the results are in line with what traditional models predict, but for large bias values, we are able to reconcile theory and data. The results for this model only depend on the bias value, and they remain valid whether or not we assume differential diffusion inside and outside the MPA.

Finally, we propose a simplified model with homogeneous diffusion everywhere, but with smooth—as opposed to piecewise constant—mortality rates. We show that once more, it is possible to unite data and theory, at least on the level of one of our measures; namely, the abundance of fish in the fishing grounds.

Our results suggest that explanations of data depend on the underlying model assumptions in a very subtle way. They seem to indicate that various explanations are possible and that further research is required to elucidate this problem.

The rest of this paper is organized as follows. In [Sect. 2](#), we present our model and show that it has a unique steady state. We examine the stability of the steady state in [Sect. 3](#). [Section 4](#) introduces various measures that quantify the effect of the MPA, and we investigate how increased mobility affects these measures. In [Sect. 5](#), we investigate a movement bias model, and in [Sect. 6](#), we consider a model with homogeneous

Fig. 1 MPAs distributed evenly along an infinite coastline



diffusion and smooth mortality. We conclude our paper in Sect. 7 with a discussion. Proofs of some of our results are in the Appendices which also contain the MATLAB code, we used for several simulations presented in the paper.

2 Model

We examine the case, where MPAs are distributed evenly and periodically along a straight coastline. The coastline can therefore be split up into several (or, in fact, infinitely many) identical sections, each containing an MPA surrounded by unprotected waters, called fishing grounds. To examine this situation, we allow one section of coastline to be represented by the interval $[-1 + 2k, 1 + 2k]$ and the MPA to be $[-l + 2k, l + 2k]$, where $0 < l < 1$ and $k \in \mathbb{Z}$, as illustrated in Fig. 1.

Assuming a completely open system, we let R represent a positive, constant recruitment rate. To describe the difference in conditions inside and outside the MPA, we assign the positive diffusion coefficient inside the MPA to be D_i and the positive diffusion coefficient outside the MPA to be D_o . We do not specify any relationship between D_i and D_o as it is not required for the following analysis. It may, however, be reasonable to choose $D_i \leq D_o$; this inequality reflects that fish diffuse more slowly in the MPA than in the fishing grounds, possibly because the protection afforded by the MPA increases the likelihood that fish will remain in the MPA for longer periods of time.

The protection afforded by the MPA also creates an important difference in mortality rates inside and outside the MPA. Namely, the mortality rate inside the MPA is lower than outside because the fish are only dying of natural causes inside the MPA while additional fish are being removed by fishers outside the MPA. Thus, we let the mortality rate inside the MPA be μ_i and the mortality rate outside the MPA be μ_o where

$$\mu_i < \mu_o.$$

Allowing the density of fish at time t and position x to be denoted by $n(x, t)$, we have the following model on an infinite coastline:

$$n_t = (D(x)n_x)_x + R - \mu(x)n \tag{1}$$

where

$$D(x) = \begin{cases} D_o & x \in (-1 + 2k, -l + 2k) \cup (l + 2k, 1 + 2k) \\ D_i & x \in (-l + 2k, l + 2k) \end{cases}$$

and

$$\mu(x) = \begin{cases} \mu_o & x \in (-1 + 2k, -l + 2k) \cup (l + 2k, 1 + 2k) \\ \mu_i & x \in (-l + 2k, l + 2k) \end{cases}$$

Using MATLAB, we can plot the solution to this system as time progresses. (Code shown in Appendix C) In Fig. 2, we can see the progression of the system (graphed on the interval $[0, 1]$, for reasons that will become clear below) through time and see the plots become more and more similar to the steady state solution calculated later in this section.

We are interested in finding steady state solutions to (1). Steady state solutions are functions $n(x)$ that are independent of t , nonnegative, continuous and which satisfy

$$0 = (D(x)n')' + R - \mu(x)n,$$

where the prime $'$ stands for d/dx . We additionally require that $n(x)$ have continuous flux and be periodic. That is, the flux $-D(x)n'(x)$ must be continuous and

$$n(x + 2) = n(x) \quad \text{for all } x \in \mathbb{R}. \tag{2}$$

Note that since $D(x)$ is discontinuous at the MPA boundaries, requiring continuous flux implies that $n'(x)$ must also be discontinuous there.

We restrict our search for steady state solutions to only those which are symmetric with respect to $x = 0$, that is, functions $n(x)$ such that

$$n(x) = n(-x) \quad \text{for all } x \text{ not on the MPA boundaries.} \tag{3}$$

These requirements create additional conditions which $n(x)$ must satisfy. To have continuous density $n(x)$ and continuous flux $-D(x)n'(x)$, we must force the left and right hand limits of these functions to match at the boundaries between the MPA and unprotected waters. Thus, we have the following matching conditions:

$$\begin{aligned} n_-(l + 2k) &= n_+(l + 2k), & n_-(-l + 2k) &= n_+(-l + 2k) \\ D_i n'_-(l + 2k) &= D_o n'_+(l + 2k), & D_o n'_-(-l + 2k) &= D_i n'_+(-l + 2k) \end{aligned} \tag{4}$$

for every $k \in \mathbb{Z}$. Here, the subscripts $-$ and $+$ indicate the left and right limit respectively.

We will show that the problem can be substantially simplified. Instead of solving the steady state equation on \mathbb{R} , it will suffice to solve the problem on $[0, 1]$ with Neumann boundary conditions.

To see this, note first that taking the derivative with respect to x in (3) yields that :

$$n'(x) = -n'(-x) \quad \text{for all } x \text{ not on the MPA boundaries.} \tag{5}$$

In particular, setting $x = 0$ implies that:

$$n'(0) = 0 \tag{6}$$

Similarly, taking derivatives in (2) and setting $x = -1$ shows that

$$n'(1) = n'(-1)$$

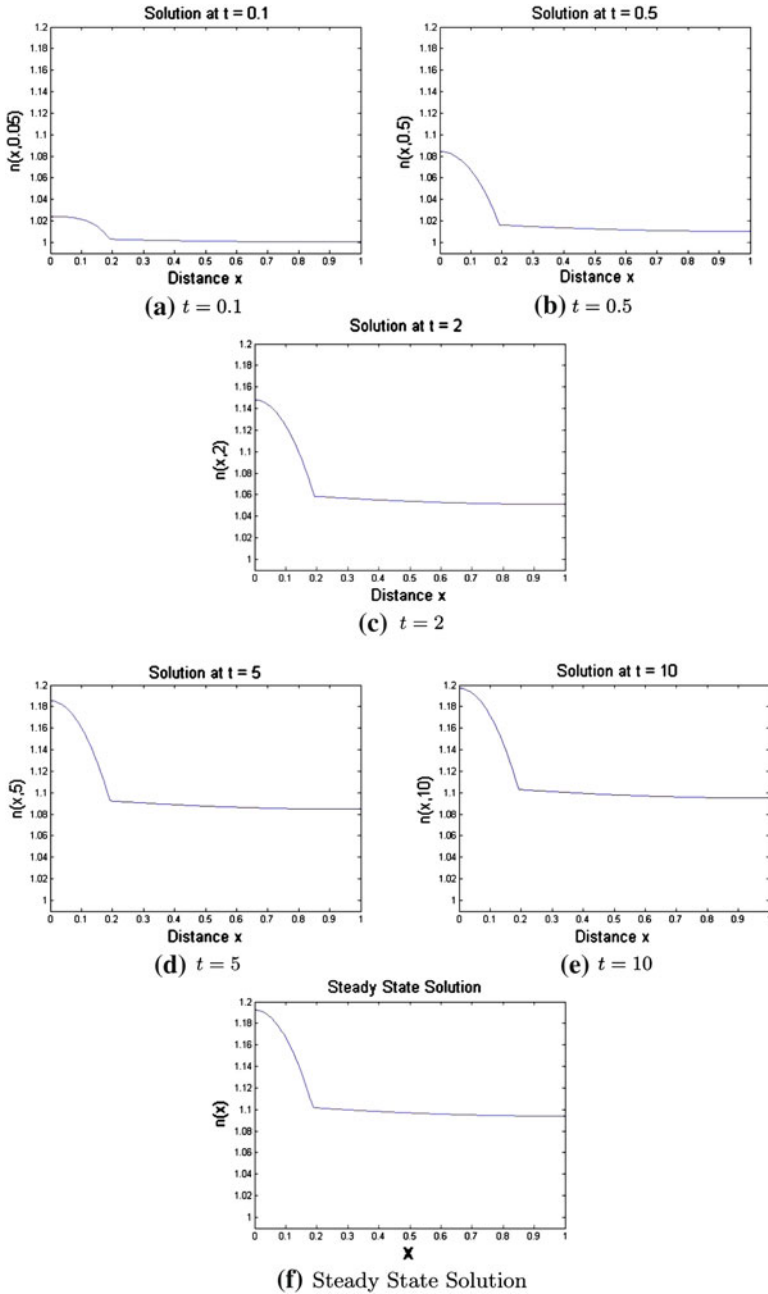


Fig. 2 Simulation of model (1). The above graphs were produced in MATLAB using the parameters $l = 3/16$ km, $D_o = 2 \frac{\text{km}^2}{\text{year}}$, $D_i = 0.04 \frac{\text{km}^2}{\text{year}}$, $R = 0.5 \frac{\text{thousands of fish}}{(\text{year})(\text{km})}$, $\mu_i = 0.25 \frac{1}{\text{year}}$, $\mu_o = 0.5 \frac{1}{\text{year}}$ and initial condition $n(x, 0) = 1 \frac{\text{thousands of fish}}{\text{km}}$ for all x . The code used can be found in Appendix C

But together with (5), evaluated at $x = 1$, this implies that

$$n'(1) = 0 \tag{7}$$

Thus, for every solution to our steady state problem, there is no flux in the points $x = 0$ and $x = 1$.

Let's assume for now (we will actually prove this below) that we can find a non-negative function $n(x)$ satisfying:

$$0 = (D(x)n')' + R - \mu(x)n, \quad x \in [0, 1] \tag{8}$$

which is continuous in $[0, 1]$, differentiable in $[0, 1]$, except perhaps in $x = l$, where the following matching conditions hold:

$$n_-(l) = n_+(l) \quad \text{and} \quad D_i n'_-(l) = D_o n'_+(l) \tag{9}$$

and with Neumann boundary conditions

$$n'(0) = n'(1) = 0 \tag{10}$$

Then it is not hard to see that the function $n(x)$ can be extended to \mathbb{R} and that the resulting extension is a solution to our original steady state problem that satisfies all the constraints we imposed. Indeed, first we extend the function $n(x)$ defined on $[0, 1]$ to $[-1, +1]$ by defining

$$n(-x) = n(x).$$

It is easily verified that this extension satisfies the steady state equation on $[-1, 0]$. Also, by the very definition of this extension, it automatically satisfies the symmetry constraint (3) on the interval $[-1, 1]$, and the matching conditions (4) at $x = -l$. Secondly, we extend this extended function $n(x)$, which is now defined on $[-1, 1]$, periodically to \mathbb{R} , by defining:

$$n(x + 2k) = n(x),$$

for all $k \in \mathbb{Z}$. It is easily verified that the resulting extension is a solution to our original problem.

What remains to be proved is the following:

Theorem 1 *The boundary-value problem (8) with (9) and (10) has a unique nonnegative solution $n(x)$ which is continuous in $[0, 1]$ and continuously differentiable in $[0, 1] \setminus \{l\}$.*

Proof Solving the equation on $[0, l)$ and $(l, 1]$ and using the Neumann boundary conditions (10), we find that:

$$n(x) = \begin{cases} c \cosh(\alpha_i x) + \frac{R}{\mu_i}, & x \in [0, l) \\ d \cosh(\alpha_o(x - 1)) + \frac{R}{\mu_o}, & x \in (l, 1] \end{cases}, \tag{11}$$

where c and d are constants determined below, and where we have introduced the following positive parameters:

$$\alpha_i = \sqrt{\frac{\mu_i}{D_i}}, \quad \alpha_o = \sqrt{\frac{\mu_o}{D_o}}. \tag{12}$$

To find c and d we use the matching condition (9):

$$\begin{aligned} c \cosh(\alpha_i l) + \frac{R}{\mu_i} &= d \cosh(\alpha_o(1-l)) + \frac{R}{\mu_o} \\ c D_i \alpha_i \sinh(\alpha_i l) &= -d D_o \alpha_o \sinh(\alpha_o(1-l)), \end{aligned}$$

or, using matrix notation:

$$\begin{pmatrix} \cosh(\alpha_i l) & -\cosh(\alpha_o(1-l)) \\ \sinh(\alpha_i l) & \frac{D_o \alpha_o}{D_i \alpha_i} \sinh(\alpha_o(1-l)) \end{pmatrix} \begin{pmatrix} c \\ d \end{pmatrix} = \begin{pmatrix} R \left(\frac{1}{\mu_o} - \frac{1}{\mu_i} \right) \\ 0 \end{pmatrix}$$

This set of equations has a unique solution if and only if the determinant of the matrix on the left, is nonzero. We calculate this determinant:

$$\begin{aligned} \Delta &= \det \begin{pmatrix} \cosh(\alpha_i l) & -\cosh(\alpha_o(1-l)) \\ \sinh(\alpha_i l) & \frac{D_o \alpha_o}{D_i \alpha_i} \sinh(\alpha_o(1-l)) \end{pmatrix} \\ &= \frac{D_o \alpha_o}{D_i \alpha_i} \cosh(\alpha_i l) \sinh(\alpha_o(1-l)) + \sinh(\alpha_i l) \cosh(\alpha_o(1-l)), \end{aligned} \tag{13}$$

and see that it is always positive, since both terms of the sum always are. The set of linear equations therefore has a unique solution:

$$\begin{pmatrix} c \\ d \end{pmatrix} = \frac{1}{\Delta} R \begin{pmatrix} \frac{1}{\mu_i} - \frac{1}{\mu_o} \\ -\frac{D_o \alpha_o}{D_i \alpha_i} \sinh(\alpha_o(1-l)) \\ \sinh(\alpha_i l) \end{pmatrix} \tag{14}$$

In particular, we see that $c < 0$ and $d > 0$. Also, notice that substituting these values of c and d back into (11), we find that the unique steady state solution is a decreasing function of x (because its derivative is negative everywhere except in $x = l$ where it is not defined, but where n is continuous).

Finally, we need to verify that $n(x) \geq 0$ for all $x \in [0, 1]$. But since $n(x)$ is decreasing, its minimal value is achieved at $x = 1$, where $n(x)$ equals $d + \frac{R}{\mu_o}$ which is positive. Thus, $n(x) \geq 0$ for all $x \in [0, 1]$ as required. \square

3 Stability of the steady state solution

The simulation in Fig. 2 suggests that the steady state $n(x)$ determined analytically in (11) with (14) is asymptotically stable. Stability properties of steady states are often established using a linearization argument. In this section, we will study the eigenvalue

problem which arises when the system is linearized at the steady state. We will show that all the eigenvalues are negative, providing further evidence of the stability of the steady state.

Linearizing model (1) at the steady state yields the following eigenvalue problem:

$$\lambda w = (D(x)w')' - \mu(x)w, \quad w'(0) = w'(1) = 0 \tag{15}$$

Solutions of this problem are eigenvalue–eigenfunction pairs $(\lambda, w(x))$ with $w(x) \neq 0$. We denote the operator on the right hand side of the Eq. (15) by $L[w]$. Its domain consists of functions w that are continuous on $[0, 1]$, with continuously differentiable flux $-D(x)w'$, and satisfying Neumann boundary condition in $x = 0$ and $x = 1$. Integration by parts shows that this operator is self-adjoint, i.e. $(L[u], v) = (u, L[v])$ for all u and v in the domain of L , where (u, v) denotes the inner product $\int_0^1 uv dx$. Consequently, the eigenvalues λ of L are real. We will prove that in fact every eigenvalue must be negative. To see this, assume that there is an eigenvalue $\lambda \geq 0$ and corresponding eigenfunction $w(x) \neq 0$, satisfying (15). Using the Neumann boundary condition, the solution $w(x)$ takes the following form:

$$w(x) = \begin{cases} A \cosh(\gamma_i x), & x \in [0, l) \\ B \cosh(\gamma_o(x - 1)), & x \in (l, 1] \end{cases},$$

where A and B are constants determined below. The parameters γ_i and γ_o are:

$$\gamma_i = \sqrt{\frac{\mu_i + \lambda}{D_i}} \text{ and } \gamma_o = \sqrt{\frac{\mu_o + \lambda}{D_o}},$$

and they are positive because $\lambda \geq 0$. To determine A and B we match the values of $w(x)$ and of the fluxes $D(x)w'(x)$ at $x = l$:

$$\begin{aligned} A \cosh(\gamma_i l) &= B \cosh(\gamma_o(l - 1)) \\ AD_i \gamma_i \sinh(\gamma_i l) &= BD_o \gamma_o \sinh(\gamma_o(l - 1)) \end{aligned}$$

Since A and B cannot be zero (otherwise $w(x)$ would be zero), we can divide both equations, which yields:

$$D_i \gamma_i \tanh(\gamma_i l) = D_o \gamma_o \tanh(\gamma_o(l - 1)).$$

But this equation cannot hold since γ_i and γ_o are positive, so that the left hand side is always positive, whereas the right hand side is always negative since $l < 1$. Thus, there cannot be an eigenvalue $\lambda \geq 0$. The absence of a nonnegative eigenvalue suggests stability.

4 Qualitative analysis of the steady state solution

To analyze the steady state solution qualitatively, we introduce and examine four quantities:

1. Fishing grounds abundance:

$$A_o = \int_l^1 n(x)dx \tag{16}$$

where $n(x)$, the steady state solution to (8) given in (11) and (14) represents the density of fish in the fishing grounds. The fishing ground abundance is the total amount of fish in the fishing grounds, at the state state.

2. Yield

$$Y = \int_l^1 (\mu_o - \mu_i) n(x)dx, \tag{17}$$

where $\mu_o - \mu_i$ represents the fishing rate. Hence, the yield represents the number of fish caught by fishers in the fishing grounds per unit of time, at the steady state.

3. The total abundance

$$A = \int_0^1 n(x)dx, \tag{18}$$

which represents the total number of fish in both the MPA and in the fishing grounds combined at the steady state.

4. The log ratio

$$L = \ln \left(\frac{\frac{1}{l} \int_0^l n(x)dx}{\frac{1}{1-l} \int_l^1 n(x)dx} \right), \tag{19}$$

the natural log of the ratio of the average abundance of fish in the MPA and in the fishing grounds evaluated at the steady state.

We are interested in what happens as both D_i and D_o increase, yet their ratio $\frac{D_i}{D_o}$ remains constant. For convenience, we define

$$D_i = D, \quad D_o = \frac{1}{\beta} D \tag{20}$$

and we let D vary, while all other parameters, including β , remain constant. We summarize the behavior of A_o , Y , A and L as functions of D as follows:

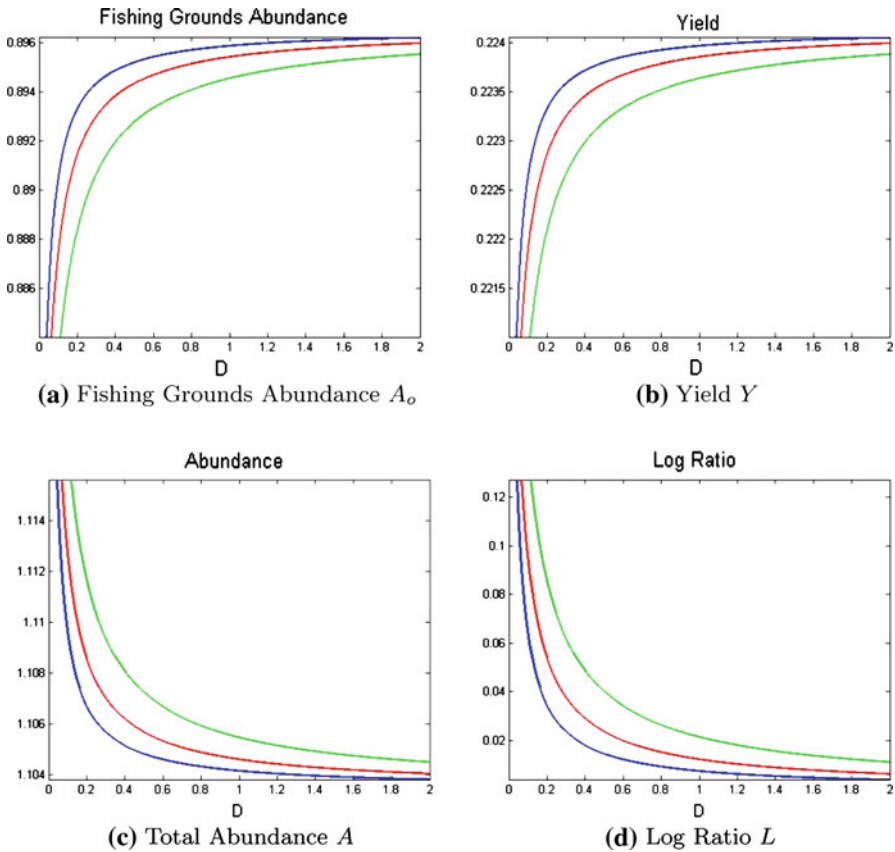


Fig. 3 The above graphs were produced in MATLAB using the parameters $l = 3/16$ km, $R = 0.5 \frac{\text{thousands of fish}}{(\text{year})(\text{km})}$, $\mu_i = 0.25 \frac{1}{\text{year}}$, $\mu_o = 0.5 \frac{1}{\text{year}}$. The values for β differ in the three plots, where $\beta = 0.5$ (top curve in **a,b**, bottom curve in **c,d**), $\beta = 1$ (middle curve in **a-d**) and $\beta = 2$ (bottom curve in **a,b**, top curve in **c,d**). The code used can be found in Appendix C

Theorem 2 Assume that (20) holds for some constant $\beta > 0$. As the diffusion coefficient D increases, the fishing grounds abundance A_o and yield Y are nondecreasing, whereas both the total abundance A and log ratio L are nonincreasing.

The proof can be found in Appendix A. Figure 3 includes graphs of these quantities for chosen parameters. We also investigated what happens if instead of the ratio, the difference of D_o and D_i remains constant, yet both increase linearly with D . The conclusions of Theorem 2 remain the same, but since the proof is very similar, it has been omitted.

5 A movement bias model

In Ovaskainen and Cornell (2003) a model is proposed that incorporates a movement bias towards the MPA. This model is obtained as the limit of a biased random walk

model. The bias occurs when the random walker is situated on the boundary of the MPA, because taking the next step towards the MPA is preferred. It is assumed that the probability to move to the right is $(1 + z)/2$, and the probability to move to the left is $(1 - z)/2$, where z takes a value in $(-1, 1)$ as a measure of the degree of bias. Note that $z = 0$ corresponds to a case without bias. When the random walker is not on the boundary, the probability of moving left or right is $1/2$. The steady state problem corresponding to the movement bias model from [Ovaskainen and Cornell \(2003\)](#), applied in the setup of an MPA, is as follows:

$$0 = (D(x)n')' + R - \mu(x)n, \quad 0 < x < 1, \quad n'(0) = n'(1) = 0, \quad (21)$$

with matching conditions:

$$(1 + z)n_-(l) = (1 - z)n_+(l) \quad \text{and} \quad D_i n'_-(l) = D_o n'_+(l) \quad (22)$$

A steady state function is any nonnegative function which is continuously differentiable, except perhaps in $x = l$, that satisfies (21) and the matching condition (22). Note that if $z \neq 0$, then necessarily n is discontinuous at $x = l$ by the first matching condition in (22). In what follows, we assume that the bias is towards the MPA, or equivalently that

$$-1 < z < 0. \quad (23)$$

Since z is negative, it follows from the first matching condition in (22) that $n_-(l)$ is always larger than $n_+(l)$, that is, the limiting values on the MPA boundary are always higher when the approach occurs within the MPA. We also note that the only difference between the steady-state problem considered in [Theorem 1](#), and the one considered here, is in the first matching condition. Nevertheless, this condition has serious impact on the behavior of the four measures considered earlier. But first, we investigate the shape of the graph of the steady state:

Theorem 3 *There is a unique nonnegative solution $n(x)$ for (21) with (22). Moreover, there is a critical bias value*

$$z^* = -\frac{\mu_o - \mu_i}{\mu_o + \mu_i}, \quad (24)$$

such that

1. If $z^* < z < 0$ (weak bias towards the MPA), then $n(x)$ is decreasing in $[0, 1]$.
2. If $z = z^*$ (critical bias), then $n(x)$ is piecewise constant with a jump discontinuity at $x = l$, given by the first matching condition in (22).
3. If $-1 < z < z^*$ (strong bias towards the MPA), then $n(x)$ is increasing in the MPA, and increasing outside the MPA.

The three cases are illustrated in [Fig. 4](#).

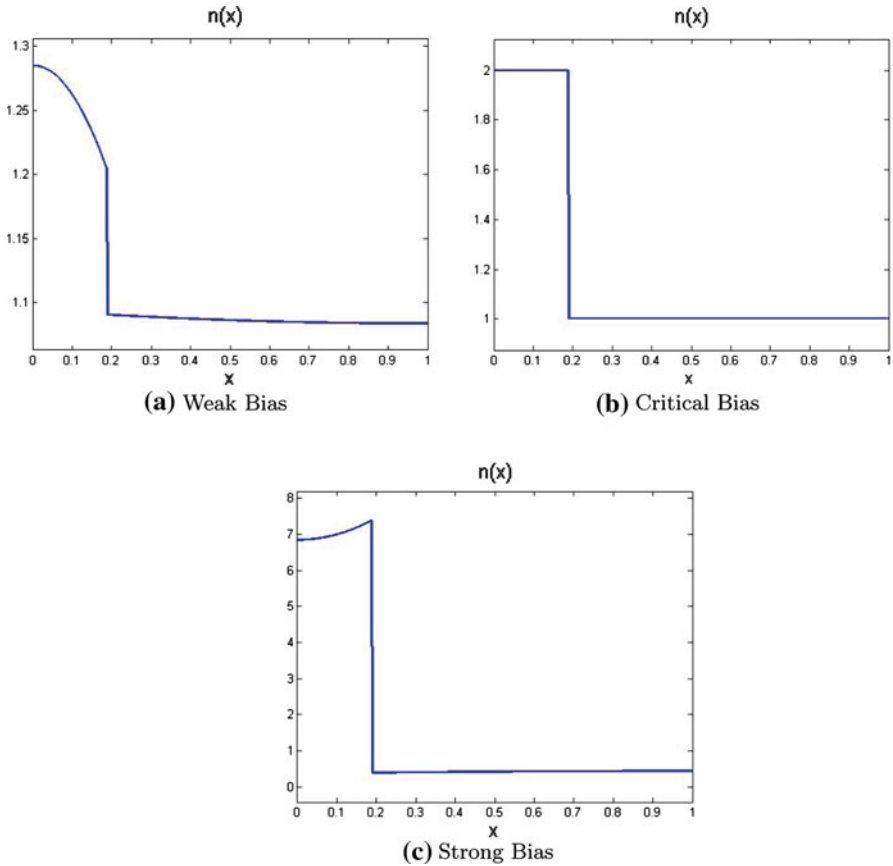


Fig. 4 The above graphs were produced in MATLAB using the parameters $l = 3/16$ km, $D_o = 2 \frac{\text{km}^2}{\text{year}}$, $D_i = 0.04 \frac{\text{km}^2}{\text{year}}$, $R = 0.5 \frac{\text{thousands of fish}}{(\text{year})(\text{km})}$, $\mu_i = 0.25 \frac{1}{\text{year}}$, $\mu_o = 0.5 \frac{1}{\text{year}}$. The plots for weak, critical and strong bias use the values $z = -0.05, -\frac{1}{3}, -0.9$, respectively. The code used can be found in Appendix C

Proof From (21) considered in the MPA and outside the MPA separately, we find that:

$$n(x) = \begin{cases} c_1 \cosh(\alpha_i x) + \frac{R}{\mu_i}, & x \in [0, l) \\ d_1 \cosh(\alpha_o(x - l)) + \frac{R}{\mu_o}, & x \in (l, 1] \end{cases} \tag{25}$$

where α_i and α_o were defined in (12), and where c_1 and d_1 are obtained using the matching condition (22):

$$\begin{pmatrix} c_1 \\ d_1 \end{pmatrix} = \frac{1}{\Delta} R(z) \begin{pmatrix} -\frac{D_o \alpha_o}{D_i \alpha_i} \sinh(\alpha_o(1 - l)) \\ \sinh(\alpha_i l) \end{pmatrix} \tag{26}$$

where

$$R(z) = \left(\frac{1}{\mu_i} - \frac{1-z}{1+z} \frac{1}{\mu_o} \right) R \tag{27}$$

and

$$\Delta = \frac{D_o \alpha_o}{D_i \alpha_i} \sinh(\alpha_o(1-l)) \cosh(\alpha_i l) + \frac{1-z}{1+z} \cosh(\alpha_o(1-l)) \sinh(\alpha_i l) \tag{28}$$

which is positive because of (23). Therefore, the sign of c_1 and d_1 is determined by the sign of $R(z)$, and the latter changes sign when z crosses z^* . This in turn implies the three distinctive cases for the shapes of the graphs of $n(x)$. Finally, we need to check that $n(x)$ is nonnegative in all three cases. For $z = z^*$ this is obvious because in this case, $n(x)$ is either equal to R/μ_i or to R/μ_o , and both values are positive. If $z^* < z$, then it suffices to check that $n(1) \geq 0$, since $n(x)$ is decreasing. But $n(1) = d_1 + R/\mu_o$, and d_1 has the same sign as $R(z)$ which is positive in this case. Similarly, if $z < z^*$, it suffices to check that $n(0) \geq 0$. But $n(0) = c_1 + R/\mu_i$ and c_1 has the same sign as $-R(z)$, which is positive as well. \square

Assuming that both D_i and D_o increase while their ratio remains constant, it turns out that, provided that the bias is weak, the monotonicity properties of the fishing grounds abundance, yield, total abundance and log ratio remain the same as in the case of the unbiased model discussed in Theorem 2. Interestingly however, when the bias is strong, the monotonicity is reversed.

Theorem 4 *Assume that (20) holds for some constant $\beta > 0$. As the diffusion coefficient D increases, the Fishing Grounds Abundance A_o and Yield Y are nondecreasing (nonincreasing), whereas both the total abundance A and log ratio L are nonincreasing (nondecreasing), provided that $z^* < z < 0$ ($-1 < z < z^*$), where z^* is given by (24).*

The proof can be found in Appendix B. Figure 5 includes graphs of these quantities for chosen parameters.

6 Constant diffusion and smooth mortality rate

In this section we show that a different model than the two models discussed before may also explain the experimental data in Claudet et al. (2010), provided the MPA size is sufficiently small. We consider a situation with constant diffusion $D > 0$ in the entire domain $[0, 1]$, and with nonconstant, positive, smooth and increasing mortality rate $\mu(x)$, say in $C^\infty[0, 1]$ with $d\mu/dx > 0$. This reflects that the values of the mortality rate are higher outside than inside the MPA due to fishing.

We consider the steady state problem:

$$Dn'' + R - \mu(x)n = 0, \quad 0 < x < 1, \quad n'(0) = n'(1) = 0. \tag{29}$$

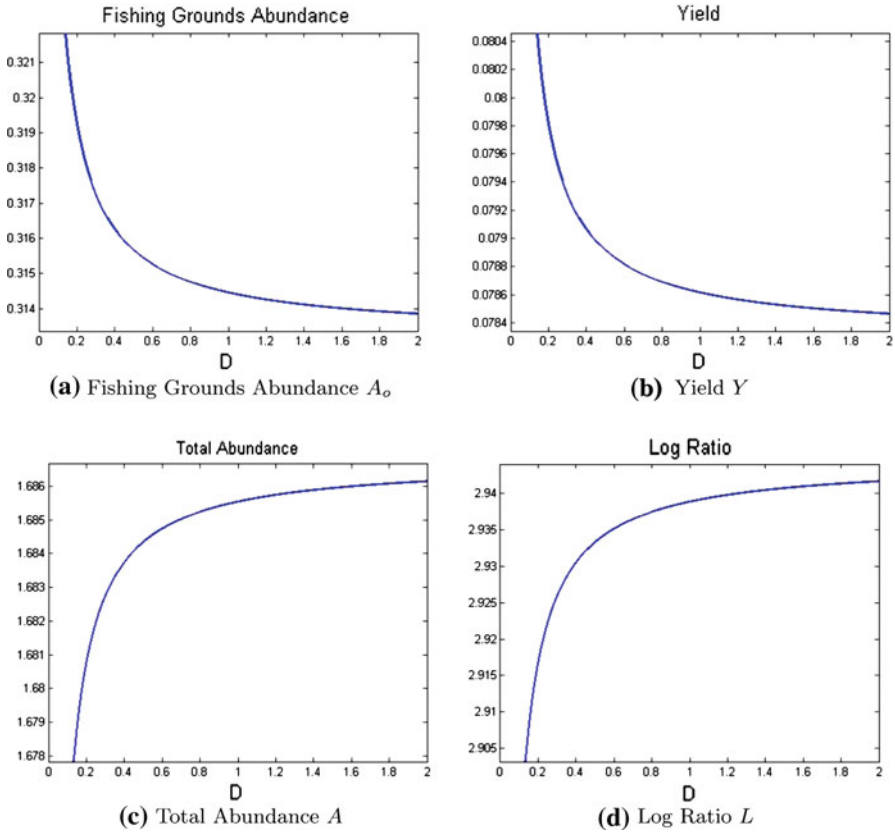


Fig. 5 The above graphs for the case of strong bias were produced in MATLAB using the parameters $l = 3/16$ km, $\beta = 0.02$, $R = 0.5 \frac{\text{thousands of fish}}{(\text{year})(\text{km})}$, $\mu_i = 0.25 \frac{1}{\text{year}}$, $\mu_o = 0.5 \frac{1}{\text{year}}$, $z = -0.9$ ($< z^* = -1/3$). The code used can be found in Appendix C

Using the methods in Sect. 3.5 from Cantrell and Cosner (2003) and cited references therein, it can be shown that (29) has a unique smooth positive solution $n(x)$ with the following properties:

$$\lim_{D \rightarrow 0} n(x) = \frac{R}{\mu(x)}, \quad \text{and} \quad \lim_{D \rightarrow \infty} n(x) = \frac{R}{\int_0^1 \mu(x) dx} \tag{30}$$

where the limits exist in $L^\infty[0, 1]$.

We investigate what happens to the fishing grounds abundance $A_o = \int_l^1 n(x) dx$ as D varies from 0 to ∞ . Contrary to what we found for the solution of model (8), (9) and (10), the fishing grounds abundance $A_o(D)$ is not necessarily nondecreasing with D as in Theorem 2, at least for sufficiently small MPA sizes:

Theorem 5 *There exists $l^* \in (0, 1)$ such that if $l < l^*$, there holds that*

$$\lim_{D \rightarrow 0} A_o(D) > \lim_{D \rightarrow \infty} A_o(D) \tag{31}$$

Proof In order to establish (31), it suffices to show that

$$\int_l^1 \frac{1}{\mu(x)} dx > \frac{1-l}{\int_0^1 \mu(x) dx} \tag{32}$$

holds, by (30). To that end, we define the following smooth auxiliary function:

$$F(l) := \left(\int_0^1 \mu(x) dx \right) \left(\int_l^1 \frac{1}{\mu(x)} dx \right) - (1-l)$$

We have that:

1. $F(0) > 0$. Indeed, this condition follows from an application of the Cauchy–Schwarz inequality in $L^2[0, 1]$ to the functions $\sqrt{\mu(x)}$ and $1/\sqrt{\mu(x)}$ (the inequality is strict because $\sqrt{\mu(x)}$ and $1/\sqrt{\mu(x)}$ are linearly independent since by assumption $\mu(x)$ is not a constant function).
2. $F(1) = 0$, which is immediate from the definition of F .
3. $\frac{dF}{dl}(1) > 0$. Indeed, we have that:

$$\frac{dF}{dl}(l) = \left(\int_0^1 \mu(x) dx \right) \left(-\frac{1}{\mu(l)} \right) + 1,$$

and since $\mu(x)$ is increasing on $[0,1]$, there holds that $\mu(x) < \mu(1)$ for $x < 1$, so that

$$\frac{dF}{dl}(1) = \left(\int_0^1 \mu(x) dx \right) \left(-\frac{1}{\mu(1)} \right) + 1 > \mu(1) \left(-\frac{1}{\mu(1)} \right) + 1 = 0.$$

These three facts imply the existence of some l^* in $(0, 1)$ such that $F(l^*) = 0$, and $F(l) > 0$ for all $l \in [0, l^*)$. But this implies that for these values of l , (32), and hence (31) holds. □

7 Discussion

Previous models suggested that increasing mobility (e.g., as reflected in an increasing diffusion parameter) would: (1) reduce the local effect of an MPA (i.e., reduce the relative disparity in density inside vs. outside of the MPA); and (2) increase the yield

(i.e., increase the catch by fishers in the unprotected region). Spillover—the movement of adults from the MPA into the fished region—contributes to both phenomena. Empirical data contradict the first expectation: more mobile fishes show a greater relative density inside of MPAs compared to more sedentary species. We hypothesize that this might be the result of ‘spill in’, driven by differential movement of fish into the MPA: i.e., if fish diffuse at different rates inside versus outside the MPA (as reflected by the parameter β in our model), then we hypothesize that increased overall movement (reflected in the parameter D) would lead to a greater buildup of fish inside the MPA.

We described movement and movement bias via a diffusion process and a discontinuity in diffusion parameters. We were able to show that our model had a unique, nonnegative, continuous steady state solution. At this steady state, as fish mobility (D) increased, abundances in the fishing grounds and yields increased, whereas total abundances and log-response ratios decreased (Fig. 3). These qualitative results were independent of the ratio β of the diffusion constants in and outside the MPA. This result is consistent with past models (using one diffusion parameter, even if these models did not calculate explicitly the log ratio, a measure commonly used in empirical studies), but it is inconsistent with the empirical results of Claudet et al. (2010). In a study of MPAs in the Florida keys, Eggleston and Parsons (2008) observed spill-in of lobster to MPAs, presumably resulting from greater movement of lobsters in the fished regions and less movement inside the MPAs. Thus, differential diffusion (as defined in our model), in the absence of movement bias, cannot explain these interesting empirical results, nor can other existing models with even simpler diffusion dynamics. However, the incorporation of a strong movement bias (Fig. 5, $z < z^*$) does resolve this paradox by reversing the expected relationships between mobility and log ratio and yield. Our description of movement bias was one of a variety of theoretical options available based on Ovaskainen and Cornell (2003). Because there are no empirical studies of movement patterns inside and outside of MPAs and at their boundary, we could not motivate our approach from relevant data.

Other assumptions likely affected our results. For example, in our first two models we assumed fishing mortality was homogeneous within the fished region (and through time), with no reallocation of fishing effort after the closure of areas to fishing pressure. Although this is a common assumption made for MPA models (e.g. Gerber et al. 2003; Pérez-Ruzafa et al. 2008; Moffitt et al. 2009), it also is well known that reallocation of fishing effort (temporal heterogeneity) can influence efficacy of MPAs Le Quesne and Codling 2009, as can ‘fishing the line’ Kellner et al. (2007), that is, increased fishing along the borders of an MPA.

In all our models we assumed a constant recruitment rate, originating from a completely open and well mixed larval pool coming from an external system unaffected by the MPA (Warner and Hughes 1988). As a consequence, the influx of new recruits was independent of local adult density or habitat. This assumption simplified our analytic approach. Other theoretical studies also assume open recruitment (Gerber et al. 2003; Rodwell et al. 2003). Others assume a totally closed system, usually described by logistic growth terms with density-dependence arising at particular points in space (e.g., via reproduction or survival: Le Quesne and Codling 2009; Baskett et al. 2005; Malvadkar and Hastings 2008; Pérez-Ruzafa et al. 2008; West et al. 2009). Assumptions about the recruitment (i.e., reaction) term can affect predicted responses to MPAs

for organisms with different rates of movement. For example, theoretical work in Lou (2006), shows that for a reaction diffusion equation with Neumann boundary condition and logistic reaction term, the total abundance A at steady state, is not monotone in terms of the spatially uniform diffusion constant D , and increases over certain ranges of D , but decreases over others. Both approaches (open and closed systems) are extreme versions of real systems and more appropriate models likely should use dispersal kernels or other distance-limited dispersal modes Moffitt et al. (2009). More research is needed to determine if our constant recruitment assumption will alter the conclusions about the qualitative effects of adult movement. Similarly, more analysis is required to establish whether the form of density-dependence affects predictions about other aspects of MPAs, including the relationship between yield and MPA size.

We have also presented a movement bias model in which the bias only occurs on the MPA boundary and nowhere else. In many other movement bias models, the bias occurs everywhere. For instance, there is a recent body of work on advection diffusion models in the theoretical ecology literature (Cantrell et al. 2007; Chen and Lou 2008). Advection may occur through different mechanisms. An obvious one is when ocean currents move fish populations, but more sophisticated ways are possible such as movement of fish in the direction of a resource gradient. Populations will crowd in regions where there are lots of resources when movement due to this advective source dominates diffusion. This is comparable to the blow-up phenomenon in chemotaxis systems Nagai et al. (1997) like the Keller–Segel model (Keller and Segel 1970), which incorporates movement of cells in the direction of a chemical substance which they secrete themselves.

Finally, following the suggestion of an anonymous reviewer, we investigated a simple model with smooth parameters. We assumed that diffusion, and recruitment are spatially uniform, but that mortality is nonuniform and monotonically increasing so that the mortality rate is higher outside than inside the MPA. It turns out that the fishing grounds abundance is not necessarily increasing with increased mobility, provided that the MPA size is small enough. This model therefore provides yet another possible explanation for the empirical data.

More targeted field research will be needed to elucidate which of these models is the more accurate one, or what modifications the models should be subject to.

Acknowledgments We thank Ben Bolker for his invaluable discussions and the Ocean Bridges Program (funded by the French-American Cultural Exchange) and the QSE3 IGERT Program (NSF award DGE-0801544) for facilitating this collaboration, which was initiated during Louise Riotte-Lambert’s internship at the University of Florida. We are also very grateful to two anonymous reviewers whose suggestions allowed us to make significant improvements to an earlier version of the paper. The first reviewer suggested that we try to establish the results in Sect. 5. The result in Sect. 6 is entirely credited to the second reviewer.

Appendix A

In this Appendix we shall prove Theorem 2. First we set $A_i = \int_0^l n(x)dx$ and $A_o = \int_l^1 n(x)dx$. Using the definition of $n(x)$ in (11) and (14), we have:

$$\begin{aligned}
 A_i &= \int_0^l n(x) dx \\
 &= \int_0^l c \cosh(\alpha_i x) + \frac{R}{\mu_i} dx \\
 &= \frac{c}{\alpha_i} \sinh(\alpha_i l) + \frac{Rl}{\mu_i} \\
 &= -\frac{R}{\Delta} \left(\frac{1}{\mu_i} - \frac{1}{\mu_o} \right) \frac{D_o \alpha_o}{D_i \alpha_i} \frac{1}{\alpha_i} \sinh(\alpha_i l) \sinh(\alpha_o(1-l)) + \frac{Rl}{\mu_i}
 \end{aligned}$$

where Δ is given by (13), and similarly for A_o :

$$\begin{aligned}
 A_o &= \int_l^1 n(x) dx \\
 &= \int_l^1 d \cosh(\alpha_o(1-x)) + \frac{R}{\mu_o} dx \\
 &= \frac{d}{\alpha_o} \sinh(\alpha_o(1-l)) + \frac{R(1-l)}{\mu_o} \\
 &= \frac{R}{\Delta} \left(\frac{1}{\mu_i} - \frac{1}{\mu_o} \right) \frac{1}{\alpha_o} \sinh(\alpha_i l) \sinh(\alpha_o(1-l)) + \frac{R(1-l)}{\mu_o}
 \end{aligned}$$

Recalling the definitions of α_i and α_o in (12), and using (20), it follows that:

$$\begin{aligned}
 A_i &= -\left(R \left(\frac{1}{\mu_i} - \frac{1}{\mu_o} \right) \frac{\sqrt{\mu_o}}{\mu_i} \right) \sqrt{\frac{D}{\beta}} \frac{\sinh\left(\sqrt{\mu_i} l \frac{1}{\sqrt{D}}\right) \sinh\left(\sqrt{\mu_o}(1-l) \sqrt{\frac{\beta}{D}}\right)}{\Delta} + \frac{Rl}{\mu_i} \\
 A_o &= \left(R \left(\frac{1}{\mu_i} - \frac{1}{\mu_o} \right) \frac{1}{\sqrt{\mu_o}} \right) \sqrt{\frac{D}{\beta}} \frac{\sinh\left(\sqrt{\mu_i} l \frac{1}{\sqrt{D}}\right) \sinh\left(\sqrt{\mu_o}(1-l) \sqrt{\frac{\beta}{D}}\right)}{\Delta} + \frac{R(1-l)}{\mu_o}
 \end{aligned}$$

and

$$\begin{aligned}
 \Delta &= \sqrt{\frac{\mu_o}{\mu_i}} \frac{1}{\sqrt{\beta}} \cosh\left(\sqrt{\mu_i} l \frac{1}{\sqrt{D}}\right) \sinh\left(\sqrt{\mu_o}(1-l) \sqrt{\frac{\beta}{D}}\right) \\
 &\quad + \sinh\left(\sqrt{\mu_i} l \frac{1}{\sqrt{D}}\right) \cosh\left(\sqrt{\mu_o}(1-l) \sqrt{\frac{\beta}{D}}\right)
 \end{aligned}$$

Defining

$$\eta_i = R \left(\frac{1}{\mu_i} - \frac{1}{\mu_o} \right) \frac{\sqrt{\mu_o}}{\mu_i}, \quad \eta_o = R \left(\frac{1}{\mu_i} - \frac{1}{\mu_o} \right) \frac{1}{\sqrt{\mu_o}}, \quad \sigma_i = \sqrt{\mu_i} l, \quad \sigma_o = \sqrt{\mu_o} (1-l),$$

we find that:

$$A_i = -\eta_i \sqrt{\frac{D}{\beta}} \frac{\sinh \left(\sigma_i \frac{1}{\sqrt{D}} \right) \sinh \left(\sigma_o \sqrt{\frac{\beta}{D}} \right)}{\Delta} + \frac{Rl}{\mu_i} \tag{33}$$

$$A_o = \eta_o \sqrt{\frac{D}{\beta}} \frac{\sinh \left(\sigma_i \frac{1}{\sqrt{D}} \right) \sinh \left(\sigma_o \sqrt{\frac{\beta}{D}} \right)}{\Delta} + \frac{R(1-l)}{\mu_o} \tag{34}$$

and

$$\Delta = \sqrt{\frac{\mu_o}{\mu_i}} \frac{1}{\sqrt{\beta}} \cosh \left(\sigma_i \frac{1}{\sqrt{D}} \right) \sinh \left(\sigma_o \sqrt{\frac{\beta}{D}} \right) + \sinh \left(\sigma_i \frac{1}{\sqrt{D}} \right) \cosh \left(\sigma_o \sqrt{\frac{\beta}{D}} \right) \tag{35}$$

The Yield Y , Total Abundance A and Log Ratio L as defined in (17), (18) and (19) respectively, can be written more compactly in terms of A_i and A_o :

$$Y = (\mu_o - \mu_i) A_o,$$

$$A = A_i + A_o,$$

and

$$L = \ln \left[\frac{(1-l)A_i}{lA_o} \right].$$

We start by examining the signs of the derivatives $\frac{dA_i}{dD}$ and $\frac{dA_o}{dD}$, and will then use this information to determine the signs of $\frac{dY}{dD}$, $\frac{dA}{dD}$ and $\frac{dL}{dD}$.

Fact:

$$\frac{dA_i}{dD} \leq 0 \text{ and } \frac{dA_o}{dD} \geq 0.$$

Before proving this, we introduce more notation.

We set $\tilde{\sigma}_o = \sigma_o \sqrt{\beta}$, $\gamma = \sqrt{\frac{\mu_o}{\mu_i \beta}}$, $\tilde{\eta}_i = \eta_i / \sqrt{\beta}$, and we let $y = \frac{1}{\sqrt{D}}$. Then we can rewrite Δ in (35) as follows:

$$\Delta = \gamma \sinh(\tilde{\sigma}_o y) \cosh(\sigma_i y) + \sinh(\sigma_i y) \cosh(\tilde{\sigma}_o y), \tag{36}$$

and (33) becomes:

$$A_i = -\tilde{\eta}_i \frac{\sinh(\tilde{\sigma}_o y) \sinh(\sigma_i y)}{\Delta y} + \frac{Rl}{\mu_i},$$

and then

$$\begin{aligned} \frac{dA_i}{dD} &= \frac{dy}{dD} \frac{dA_i}{dy} \\ &= -\tilde{\eta}_i \frac{y^3}{2} \frac{d}{dy} \left[\frac{\sinh(\tilde{\sigma}_o y) \sinh(\sigma_i y)}{\Delta y} \right] \\ &= \tilde{\eta}_i \frac{y^3}{2} \frac{(\tilde{\sigma}_o \cosh(\tilde{\sigma}_o y) \sinh(\sigma_i y) + \sigma_i \sinh(\tilde{\sigma}_o y) \cosh(\sigma_i y)) (\Delta y) - \sinh(\tilde{\sigma}_o y) \sinh(\sigma_i y) \left(y \frac{d\Delta}{dy} + \Delta \right)}{(\Delta y)^2} \\ &= \tilde{\eta}_i \frac{y}{2\Delta^2} f(y), \end{aligned}$$

where we used (36) in the last step and introduced

$$\begin{aligned} f(y) &:= \sinh^2(\sigma_i y) [\tilde{\sigma}_o y - \sinh(\tilde{\sigma}_o y) \cosh(\tilde{\sigma}_o y)] \\ &\quad + \gamma \sinh^2(\tilde{\sigma}_o y) [\sigma_i y - \sinh(\sigma_i y) \cosh(\sigma_i y)]. \end{aligned} \tag{37}$$

Thus, the sign of $\frac{dA_i}{dD}$ is equal to the sign of $f(y)$. To determine this, we examine the function $a - \sinh(a) \cosh(a) = a - \frac{1}{2} \sinh(2a)$ for $a \geq 0$. Note that when $a = 0$, $\frac{1}{2} \sinh(2a) = 0$ and that $\frac{d}{da} (a - \frac{1}{2} \sinh(2a)) = 1 - \cosh(2a) = \frac{d}{da} (\frac{1}{2} \sinh(2a))$ for $a \geq 0$. Thus, $a \leq \frac{1}{2} \sinh(2a)$ for all $a \geq 0$ and consequently (37) is nonpositive for $y > 0$. This shows that $\frac{dA_i}{dD} \leq 0$.

We use a similar calculation for A_o . Setting $\tilde{\eta}_o = \eta_o / \sqrt{\beta}$, we rewrite A_o as

$$A_o = \tilde{\eta}_o \frac{\sinh(\tilde{\sigma}_o y) \sinh(\sigma_i y)}{\Delta y} + \frac{R(1-l)}{\mu_o}.$$

Then

$$\begin{aligned} \frac{dA_o}{dD} &= \frac{dy}{dD} \frac{dA_o}{dy} \\ &= \tilde{\eta}_o \frac{y^3}{2} \frac{d}{dy} \left[\frac{\sinh(\tilde{\sigma}_o y) \sinh(\sigma_i y)}{\Delta y} \right] \\ &= -\tilde{\eta}_o \frac{y}{2\Delta^2} f(y) \\ &\geq 0 \text{ for all } y > 0. \end{aligned}$$

Proof of Theorem 2 1. $\frac{dA_o}{dD} \geq 0$. This has already been shown.

2. $\frac{dY}{dD} \geq 0$. Indeed, since $Y = (\mu_o - \mu_i)A_o$ and $\frac{dA_o}{dD} \geq 0$, it follows that

$$\frac{dY}{dD} = 2(\mu_o - \mu_i) \frac{dA_o}{dD} \geq 0.$$

3. $\frac{dA}{dD} \leq 0$.

Since $A = A_i + A_o$, it follows that

$$\begin{aligned} \frac{dA}{dD} &= \left(\frac{dA_i}{dD} + \frac{dA_o}{dD} \right) \\ &= \left(\tilde{\eta}_i \frac{1}{2\sqrt{D}\Delta^2} f\left(1/\sqrt{D}\right) - \tilde{\eta}_o \frac{1}{2\sqrt{D}\Delta^2} f\left(1/\sqrt{D}\right) \right) \\ &= \frac{1}{2\sqrt{D}\Delta^2} (\eta_i - \eta_o) f\left(\sqrt{D}\right) \end{aligned}$$

Recall from (37) that $f(y) \leq 0$ if $y > 0$. Moreover,

$$\tilde{\eta}_i - \tilde{\eta}_o = \frac{R}{\sqrt{\beta}} \left(\frac{1}{\mu_i} - \frac{1}{\mu_o} \right) \left(\frac{\mu_o - \mu_i}{\mu_i \sqrt{\mu_o}} \right) > 0,$$

and therefore $\frac{dA}{dD} \leq 0$.

4. $\frac{dL}{dD} \leq 0$.

Notice that

$$\begin{aligned} L &= \ln \left[\frac{(1-l)A_i}{lA_o} \right] \\ &= \ln \left[\frac{1-l}{l} \right] + \ln \left[\frac{A_i}{A_o} \right]. \end{aligned}$$

Moreover,

$$\frac{A_i}{A_o} = \frac{\int_0^l n(x)dx}{\int_l^1 n(x)dx} = \frac{\int_0^1 n(x)dx}{\int_l^1 n(x)dx} - 1 = \frac{A}{Y/(\mu_0 - \mu_i)} - 1$$

Since A is nonincreasing and Y is nondecreasing with D , it follows that A_i/A_o and hence L is nonincreasing with D .

Appendix B

Here we only sketch part of the proof of Theorem 4, as it is similar to that of Theorem 2.

Since $A_i = \int_0^l n(x)dx$, and $n(x)$ is given by (25), with (26), there holds that

$$A_i = -\frac{D_o\alpha_o}{D_i\alpha_i^2\Delta} \sinh(\alpha_o(1-l)) \sinh(\alpha_i l) R(z) + \frac{Rl}{\mu_i}$$

where $R(z)$ is given by (27), and Δ by (28). By (20), recalling (12) and setting $\tilde{\sigma}_o = \sqrt{\mu_o}(1-l)\sqrt{\beta}$ and $\sigma_i = \sqrt{\mu_i}l$, it follows that

$$A_i = -\frac{\sqrt{\mu_o}}{\mu_i\sqrt{\beta}} \frac{\sinh(\tilde{\sigma}_o y) \sinh(\sigma_i y)}{\Delta y} R(z) + \frac{Rl}{\mu_i}$$

where as before, we have set $y = 1/\sqrt{D}$, and where:

$$\Delta = \gamma \sinh(\tilde{\sigma}_o y) \cosh(\sigma_i y) + \frac{1-z}{1+z} \cosh(\tilde{\sigma}_o y) \sinh(\sigma_i y)$$

with $\gamma = \sqrt{\mu_o/(\beta\mu_i)}$. Therefore,

$$\frac{dA_i}{dD} = \frac{dy}{dD} \frac{dA_i}{dy} = +\frac{\sqrt{\mu_o}}{\mu_i\sqrt{\beta}} \frac{y^3}{2} R(z) \frac{d}{dy} \left[\frac{\sinh(\tilde{\sigma}_o y) \sinh(\sigma_i y)}{\Delta y} \right]$$

Proceeding similarly as in the proof of Theorem 2, but being cautious because now the factor $(1-z)/(1+z)$ appears in the second term of Δ here, it follows that:

$$\frac{dA_i}{dD} = +\frac{\sqrt{\mu_o}}{\mu_i\sqrt{\beta}} \frac{y}{2\Delta^2} R(z) \left[\gamma \sinh^2(\tilde{\sigma}_o y)g(\sigma_i y) + \frac{1-z}{1+z} \sinh^2(\sigma_i y)g(\tilde{\sigma}_o y) \right],$$

where

$$g(x) = x - \sinh(x) \cosh(x).$$

Since $g(x) \leq 0$ if $x \geq 0$, it follows that the sign of dA_i/dD is opposite to the sign of $R(z)$ ($R(z)$ is defined in (27)). As the latter is negative if $z < z^*$, zero if $z = z^*$, and positive if $z > z^*$, it follows that

$$\frac{dA_i}{dD} \begin{cases} < 0, & \text{if } z > z^* \text{ (weak bias)} \\ = 0, & \text{if } z = z^* \text{ (critical bias)} \\ > 0, & \text{if } z < z^* \text{ (strong bias)} \end{cases}$$

In particular, we notice that the sign of dA_i/dD is reversed when z moves from weak bias values to strong ones. We omit the rest of the proof of the Theorem 4 as it is similar to that of Theorem 2.

Appendix C

In this Appendix we provide the MATLAB code that was used to simulate System (1) for $t \geq 0$, and the four measures and steady state for the various models.

The following code was used to generate the simulation of System (1) for chosen $t \geq 0$ in Fig. 2.

```

function MPAplot
%This m file is to plot the {MPA} system (with recruitment R) after a
%specified number of time steps

%see help file for {pdepe}

m = 0;
x = linspace(0,1,100);
%Time
t = linspace(0,10,100);

sol = pdepe(m,@MPAplotpde,@MPAplotic,@MPAplotbc,x,t);
% Extract the first solution component as u.
u = sol(:,:,1);

% Solution profile:
figure
plot(x,u(end,:))
xlabel('Distance x')
ylabel('n(x,10)')
% -----
function [c,f,s] = MPAplotpde(x,t,u,DuDx)
l = 3/16;
b=0.02;
Di = 0.04;
Do = Di/b;
R = 0.5;
mi = 0.25;
mo = 0.5;

if x<l
    h = 0;
else
    h = 1;
end

D = Di + (Do-Di)*h;
mu = mi + (mo-mi)*h;

c = 1;
f = D*DuDx;
s = R-mu*u;
% -----
function u0 = MPAplotic(x)
R = 0.5;
mo = 0.5;

u0 = R/mo;
% -----
function [pl,ql,pr,qr] = MPAplotbc(xl,ul,xr,ur,t)
b=0.02;
Di = 0.04;
Do = Di/b;

```

```

p1 = 0;
q1 = 1/Di;
pr = 0;
qr = 1/Do;
%-----

```

The following code was used to generate the steady state solution of System (1) for $t \geq 0$ in Fig. 2.

```

function symbolic2

syms x

l = 3/16;
Di = 0.04;
Do = 2;
b = Di/Do;
R = 0.5;
mi = 0.25;
mo = 0.5;
ai = sqrt(mi/Di);
ao = sqrt(mo/Do);
%p = Delta
p = sqrt(mo/(b*mi))*sinh(ao*(1-l))*cosh(ai*l)
    + sinh(ai*l)*cosh(ao*(1-l));
c = (1/p)*R*(mo-mi)/(mo*mi)*sqrt(mo/(b*mi))*(-1)
    *sinh(ao*(1-l));
d = (1/p)*R*(mo-mi)/(mo*mi)*sinh(ai*l);
ni = c*cosh(ai*x) + (R/mi);
no = d*cosh(ao*(1-x)) + (R/mo);
n = ni + heaviside(x-1)*(no-ni);

p0 = ezplot(n, [0, 1]);
set(p0,'Color','blue','LineWidth', 2);
%-----

```

The following code was used to generate Fig. 3.

```

function symbolic
syms x D

l = 3/16;
b = [.5 1 2];
R = 0.5;
mi = 0.25;
mo = 0.5;

for i=1:3
    ai(i) = sqrt(mi/D);

```

```

end
for i=1:3
    ao(i) = sqrt(b(i)*mo/D);
end

%p = Delta
for i=1:3
    p(i) = sqrt(mo/(b(i)*mi))*sinh(ao(i)*(1-l))
        *cosh(ai(i)*l) + sinh(ai(i)*l)
        *cosh(ao(i)*(1-l));
end

for i=1:3
    c(i) = (1/p(i))*R*(mo-mi)/(mo*mi)*sqrt(mo/(b(i)*mi))
        *(-1)*sinh(ao(i)*(1-l));
end

for i=1:3
    d(i) = (1/p(i))*R*(mo-mi)/(mo*mi)*sinh(ai(i)*l);
end

for i=1:3
    ni(i) = c(i)*cosh(ai(i)*x) + (R/mi);
end

for i=1:3
    no(i) = d(i)*cosh(ao(i)*(1-x)) + (R/mo);
end

for i=1:3
    Ii(i) = int(ni(i),x,0,l);
end

for i=1:3
    Io(i) = int(no(i),x,l,1);
end

for i=1:3
    Y(i) = (mo-mi)*Io(i) ;
end

for i=1:3
    A(i) = (Ii(i)+Io(i));
end

```

```
for i=1:3
    L(i) = log(((1-l)*Ii(i))/(l*Io(i)));
end

for i=1:3
    n(i) = ni(i) + heaviside(x-l)*(no(i)-ni(i));
end

p0 = ezplot(A(1), [0, 2]);
set(p0,'Color','blue', 'LineWidth', 2);
hold on;
p1 = ezplot(A(2), [0, 2]);
set(p1,'Color','red', 'LineWidth', 2);
p2 = ezplot(A(3), [0, 2]);
set(p2,'Color','green', 'LineWidth', 2);
hold off
%-----
```

The following code was used to generate Fig. 4.

```
function bias

syms x

l = 3/16;
b = 0.02;
Di = 0.04;
Do = Di/b;
z = [-.05 -1/3 -.9];
R0 = 0.5;
mi = 0.25;
mo = 0.5;

ai = sqrt(mi/Di);
ao = sqrt(mo/Do);

for i=1:3
    R(i) = R0* ((1/mi) - (1-z(i))/(1+z(i))/mo);
end

%p = Delta
for i=1:3
    p(i) = (Do*ao)/(Di*ai)*sinh(ao*(1-l))*cosh(ai*l)
           +(1-z(i))/(1+z(i))*sinh(ai*l)*cosh(ao*(1-l));
end
```

```

for i=1:3
    c(i) = -(1/p(i))*R(i)*(Do*ao)/(Di*ai)
           *sinh(ao*(1-l));
end

for i=1:3
    d(i) = (1/p(i))*R(i)*sinh(ai*1);
end

for i=1:3
    ni(i) = c(i)*cosh(ai*x) + (R0/mi);
end

for i=1:3
    no(i) = d(i)*cosh(ao*(1-x)) + (R0/mo);
end

for i=1:3
    Ii(i) = int(ni(i),x,0,1);
end

for i=1:3
    Io(i) = int(no(i),x,1,1);
end

for i=1:3
    Yi(i) = (mo-mi)*Io(i) ;
end

for i=1:3
    Ai(i) = (Ii(i)+Io(i));
end

for i=1:3
    Li(i) = log(((1-l)*Ii(i))/(l*Io(i)));
end

for i=1:3
    n(i) = ni(i) + heaviside(x-1)*(no(i)-ni(i));
end

p0 = ezplot(n(3), [0, 1]);
set(p0,'Color','blue', 'LineWidth', 2);
%-----

```

The following code was used to generate Fig. 5.

```

function bias2

syms x D

l = 3/16;
b = 0.02;
Do = D/b;
%Dl = D;
z = -.9;
R0 = 0.5;
mi = 0.25;
mo = 0.5;

ai = sqrt(mi/D);
ao = sqrt(mo/Do);

R = R0* ((1/mi) - (1-z)/(1+z)/mo);
%p = Delta
p = (Do*ao)/(D*ai)*sinh(ao*(1-l))*cosh(ai*l)
    +(1-z)/(1+z)*sinh(ai*l)*cosh(ao*(1-l));
c = -(1/p)*R*(Do*ao)/(D*ai)*sinh(ao*(1-l));
d = (1/p)*R*sinh(ai*l);
ni = c*cosh(ai*x) + (R0/mi);
no = d*cosh(ao*(1-x)) + (R0/mo);
Ii = int(ni,x,0,l);
Io = int(no,x,l,1);
Y = (mo-mi)*Io ;
A = (Ii+Io);
L = log(((1-l)*Ii)/(l*Io));

p0 = ezplot(L, [0, 2]);
set(p0,'Color','blue','LineWidth', 2);

```

References

- Baskett ML, Levin SA, Gaines SD, Dushoff J (2005) Marine reserve design and the evolution of size at maturation in harvested fish. *Ecol Appl* 15:882–901
- Cantrell RS, Cosner C (1999) Diffusion models for population dynamics incorporating individual behavior at boundaries: applications to refuge design. *Theor Popul Biol* 55:189–207
- Cantrell RS, Cosner C, Lou Y (2007) Advection-mediated coexistence of competing species. *Proc R Soc Edinburgh* 137A:487–518
- Cantrell RS, Cosner C (2003) Spatial ecology via reaction–diffusion equations. Wiley, New York
- Chen X, Lou Y (2008) Principal Eigenvalue and Eigenfunctions of an elliptic operator with large advection and its application to a competition model. *Indiana Univ Math J* 57:627–658
- Claudet J, Osenberg CW, Benedetti-Cecchi L, Domenici P, Garcia-Charton JA, Perez-Ruzafa A, Badalamenti F, Bayle-Sempere J, Brito A, Bulleri F, Culioli JM, Dimech M, Falcón JM, Guala I, Milazzo M, Sánchez-Meca J, Somerfield PJ, Stobart B, Vandeperre F, Valle C, Planes S (2008) Marine reserves: size and age do matter. *Ecol Lett* 11:481–489

- Claudet J, Osenberg CW, Domenici P, Badalamenti F, Milazzo M, Falcón JM, Bertocci I, Benedetti-Cecchi L, Garcia-Charton J-A, Goñi R, Borg JA, Forcada A, De Lucia A, Pérez-Ruzafa A, Afonso P, Brito A, Guala I, Le Diréach L, Sanchez-Jerez P, Somerfield PJ, Planes S (2010) Marine reserves: fish life history and ecological traits matter. *Ecol Appl* 20:830–839
- Eggleston DB, Parsons DM (2008) Disturbance-induced 'spill-in' of Caribbean lobster to marine reserves. *Mar Ecol Prog Ser* 371:213–220
- Gerber LR, Botsford LW, Hastings A, Possingham HP, Gaines SD, Palumbi SR, Andelman S (2003) Population models for marine reserve design: a retrospective and prospective synthesis. *Ecol Appl* 13:47–64
- Goñi R, Adlerstein S, Alvarez-Berastegui D, Forcada A, Reñones O, Criquet G, Polti S, Cadiou G, Valle C, Lenfant P, Bonhomme P, Pérez-Ruzafa A, Sánchez-Lizaso FL, García-Charton JA, Bernard G, Stelzenmüller V, Planes S (2008) Spillover from six western Mediterranean marine protected areas: evidence from artisanal fisheries. *Mar Ecol Prog Ser* 366:159–174
- Halpern BS (2003) The impact of marine reserves: do reserves work and does reserve size matter? *Ecol Appl* 13:117–137
- Hilborn R, Stokes K, Maguire JJ, Smith T, Botsford LW, Mangel M, Orensanz J, Parma A, Rice J, Bell J, Cochrane KL, Garcia S, Hall SJ, Kirkwood GP, Sainsbury K, Stefansson G, Walters C (2004) When can marine reserves improve fisheries management? *Ocean Coast Manage* 47:197–205
- Keller EF, Segel LA (1970) Initiation of slime mold aggregation viewed as an instability. *J Theor Biol* 26:399–415
- Kellner JB, Tetreault I, Gaines SD, Nisbet RM (2007) Fishing the line near marine reserves in single and multispecies fisheries. *Ecol Appl* 17:1039–1054
- Le Quesne WJF, Codling EA (2009) Managing mobile species with MPAs: the effects of mobility, larval dispersal, and fishing mortality on closure size. *ICES J Mar Sci* 66:122–131
- Lou Y (2006) On the effects of migration and spatial heterogeneity on single and multiple species. *J Differ Equ* 223:400–426
- Malvadkar U, Hastings A (2008) Persistence of mobile species in marine protected areas. *Fish Res* 91:69–78
- Moffitt EA, Botsford LW, Kaplan DM, O'Farrell MR (2009) Marine reserve networks for species that move within a home range. *Ecol Appl* 19:1835–1847
- Nagai T, Senba T, Yoshida K (1997) Application of the Trudinger–Moser inequality to a parabolic system of chemotaxis. *Funkcilaj Ekvacioj* 40:411–433
- Osenberg CW, Bolker BM, White JS, St. Mary C, Shima JS (2006) Statistical issues and study design in ecological restorations: lessons learned from marine reserves. In: Falk D, Palmer N, Zedler J (eds) *Foundations of restoration ecology*. Island Press, Washington, DC pp 280–302
- Ovaskainen O, Cornell SJ (2003) Biased movement at a boundary and conditional occupancy times for diffusion processes. *J Appl Probability* 40:557–580
- Pérez-Ruzafa A, Martín E, Marcos C, Zamarro JM, Stobart B, Harmelin-Vivien M, Polti S, Planes S, García-Charton JA, González-Wangüemert M (2008) Modeling spatial and temporal scales for spillover and biomass exportation from MPAs and their potential for fisheries enhancement. *J Nat Conserv* 16:234–255
- Roberts CM, Bohnsack JA, Gell F, Hawkins JP, Goodridge R (2001) Effects of marine reserves on adjacent fisheries. *Science* 294:1920–1923
- Rodwell LD, Barbier EB, Roberts CM, McClanahan TR (2003) The importance of habitat quality for marine reserve-fishery linkages. *Can J Fisheries Aquat Sci* 60:171–181
- Sale PF, Cowen RK, Danilowicz BS, Jones GP, Kritzer JP, Lindeman KC, Planes S, Polunin NVC, Russ GR, Sadovy YJ, Steneck RS (2005) Critical science gaps impede use of no-take fishery reserves. *Trends Ecol Evol* 20:74–80
- Selig ER, Bruno JF (2010) A global analysis of the effectiveness of marine protected areas in preventing coral loss. *PLoS ONE* 5
- Shigesada N, Kawasaki K, Teramoto E (1986) Traveling periodic waves in heterogeneous environments. *Theor Popul Biol* 30:143–160
- Warner RR, Hughes TP (1988) The population dynamics of reef fishes. In: *Proceedings of 6th international coral reef symposium, vol 1*. Townsville, pp 146–155
- West CD, Dytham C, Righton D, Pitchford JW (2009) Preventing overexploitation of migratory fish stocks: the efficacy of marine protected areas in a stochastic environment. *ICES J Mar Sci* 66:1919–1930